

Article

# Formation and Application of High Reflectivity Controllable Barium Sulfate Microspheres

Yuejiao Liu <sup>1,2</sup>, Xiaoyan Guo <sup>1</sup>, Qingyang Gu <sup>1</sup>, Guangxiang He <sup>1</sup> , Suohe Yang <sup>1</sup> and Haibo Jin <sup>1,\*</sup> 

<sup>1</sup> Beijing Key Laboratory of Fuels Cleaning and Advanced Catalytic Emission Reduction Technology, Department of Chemical Engineering, Beijing Institute of Petrochemical Technology, Beijing 102617, China; 5320150108@bipt.edu.cn (Y.L.); guoxiaoyan@bipt.edu.cn (X.G.); guqingyang@bipt.edu.cn (Q.G.); hgx@bipt.edu.cn (G.H.); yangsuohe@bipt.edu.cn (S.Y.)

<sup>2</sup> Department of Chemical Engineering, Beijing University of Chemical Technology, Beijing 100028, China

\* Correspondence: jinhaibo@bipt.edu.cn; Tel.: +86-10-81292208

Received: 7 July 2018; Accepted: 31 July 2018; Published: 21 August 2018



**Abstract:** This paper investigated the influence of reaction conditions on particle morphology. X-ray powder diffraction (XRD), particle size distribution (PSD), and scanning electron microscopy (SEM) were used to characterize the morphology of barium sulfate. The barium sulfate microspheres were synthesized with BaCl<sub>2</sub>, Na<sub>2</sub>SO<sub>4</sub>, and ethylenediaminetetraacetic acid disodium (EDTA·2Na). The reflectivity of the synthesized barium sulfate microspheres was greater than 99% in the range of 400–700 nm, which was characterized by a reflectance spectrometer. The morphology of the barium sulfate particles and their cross-section were observed by SEM. The prepared microspheres were applied to high-density lipoprotein dry tablets due to their high reflectivity, and the results showed that the prepared tablets had high sensitivity and good repeatability.

**Keywords:** barium sulfate; ethylenediaminetetraacetic acid disodium (EDTA); microspheres; high-density lipoprotein

## 1. Introduction

With excellent physicochemical characteristics, e.g., non-toxicity, acid and alkali resistance, high reflectivity, and high whiteness, barium sulfate (BaSO<sub>4</sub>) has been widely used in pigment filling, in ceramics, as a catalyst carrier [1], an adsorbent [2], a medical contrast agent [3], an additive in polymers and [4,5], and in other fields. In addition, barium sulfate particles with complex structures, such as fiber bundles [6], peanuts [7], and almonds [8], have been synthesized. The morphology and particle size of barium sulfate determine its application path. The homogeneous particle size of BaSO<sub>4</sub> microspheres has the advantage of high light reflectivity [9], and the accumulated voids can effectively and uniformly disperse a serum and achieve filtration separation [10,11]. Therefore, BaSO<sub>4</sub> microspheres can be used as a filtration-diffusion-reflection multifunctional layer for medical dry diagnostic reagents. This subject is presently one of the research hotspots and it is one of the key technologies being used to prepare the uniform particle size of micron-sized BaSO<sub>4</sub> in the field of medical dry diagnostics.

In this study, the industrial synthesis methods of barium sulfate mainly include physical and chemical methods. The surface of spheroid particles prepared by the physical method is irregular and widely distributed [12]. The resulting diffusion layer generates diffuse reflection on light, thus making the coating dull. New chemical production methods of barium sulfate mainly include the following: (1) Li et al. [13] used sodium polypropionate (PAA) to synthesize barium micron spherical sulfate. They defined the interaction mechanism between the PAA carboxyl group and inorganic ions and

the conformational changes of the PAA molecular chain affecting the morphology of barium sulfate. Sodium polyacrylate is not suitable for mass production because of its high price. (2) Wang et al. [14] prepared barium sulfate nanoparticles with a diameter of 10–90 nm by the microemulsion method. A large number of organic solvents and surfactants were used in the experiment, resulting in a large number of impurities in the product. (3) Liu et al. [15] prepared barium sulfate particles by complexation. Uchida et al. [16,17] prepared needle-like barium sulfate nanoparticles by complexation. It has been widely used as an important complexing agent [18–22].

A new type of barium sulfate microsphere was synthesized by using ethylenediaminetetraacetic acid (EDTA) as the complexing agent to control barium sulfate precipitation. The morphology of barium sulfate particles was characterized by X-ray powder diffraction (XRD) and scanning electron microscopy (SEM). The synthesized barium sulfate microsphere was used to prepare high-density lipoprotein dry tablets with high sensitivity and repeatability.

## 2. Materials and Methods

### 2.1. Materials

Barium chloride (A.R., grade, Sinopharm Group, Beijing, China), EDTA.2Na (A.R., grade, Sinopharm Group, Beijing, China), NaOH (A.R., grade, Beijing Hengye Zhongyun Chemical Industry, Beijing, China), sodium sulfate (A.R., grade, Sinopharm Group, Beijing, China), hydrochloric acid (36–38%, grade, Beijing Chemical Plant, Beijing, China), sodium persulfate (A.R., grade, Sinopharm Group, Beijing, China), deionized water.

### 2.2. Methods

Under the conditions of constant temperature and stirring, the EDTA and BaCl<sub>2</sub> were mixed evenly and then the pH was adjusted with a sodium hydroxide solution. When the pH of the solution was stable, Na<sub>2</sub>SO<sub>4</sub> or Na<sub>2</sub>S<sub>2</sub>O<sub>8</sub> was added. When the reaction was complete, the product was washed several times with deionized water and ethanol.

## 3. Results

### 3.1. Preparation of Barium Sulfate Microspheres

#### 3.1.1. Influence of EDTA

In processes involving barium sulfate particles, EDTA plays an important role that affects not only the free Ba<sup>2+</sup> content in the solution, but also directly affects the morphology of BaSO<sub>4</sub> particles [23]. Barium sulfate particles synthesized with BaCl<sub>2</sub> and Na<sub>2</sub>SO<sub>4</sub> are shown in Figure 1A. The product was composed of amorphous flat particles, similar to the morphology reported in the literature [24]. BaSO<sub>4</sub> particles obtained with EDTA were transformed from amorphous to microspheres, as shown in Figure 1B. The reason for this phenomenon was that the EDTA complexing agent controlled the over-saturation of Ba<sup>2+</sup> in the solution to achieve homogeneous nucleation, so as to synthesize barium sulfate with a uniform particle size. The image of barium sulfate synthesized with BaCl<sub>2</sub> and Na<sub>2</sub>S<sub>2</sub>O<sub>8</sub> shows irregular square lamella particles, as shown in Figure 1C. Although Na<sub>2</sub>S<sub>2</sub>O<sub>8</sub> can control the release of SO<sub>4</sub><sup>2-</sup> in solution, it cannot slowly react to form microspheres. This phenomenon further proves that EDTA not only controls the concentration of Ba<sup>2+</sup> in solution, but also plays an important role in the formation of barium sulfate microspheres. Figure 2 shows the XRD patterns of barium sulfate particles at different conditions, respectively. All diffracted lines in Figure 2 could correspond to orthogonal crystal barium sulfate (Joint Committee on Powder Diffraction Standards, JCPDS No. 24–1035). As we can see from Figure 2a, the diffraction line is very sharp and strong, indicating that the resulting sample has a high crystallinity. The BaSO<sub>4</sub> synthesized with the EDTA in Figure 2b shows a diffraction line with a Scherrer broadening, and the crystal is considered to be smaller compared to Figure 2a. The peak height of XRD indicates that barium sulfate particles have different sizes of

structural units. The reduction of the barium sulfate structural units prepared by  $\text{BaCl}_2$ ,  $\text{Na}_2\text{SO}_4$ , and EDTA complexants is due to the adsorption of EDTA on the surface of the  $\text{BaSO}_4$  nucleus, which hinders the growth of the  $\text{BaSO}_4$  nucleus and is conducive to the formation of nanoparticles.

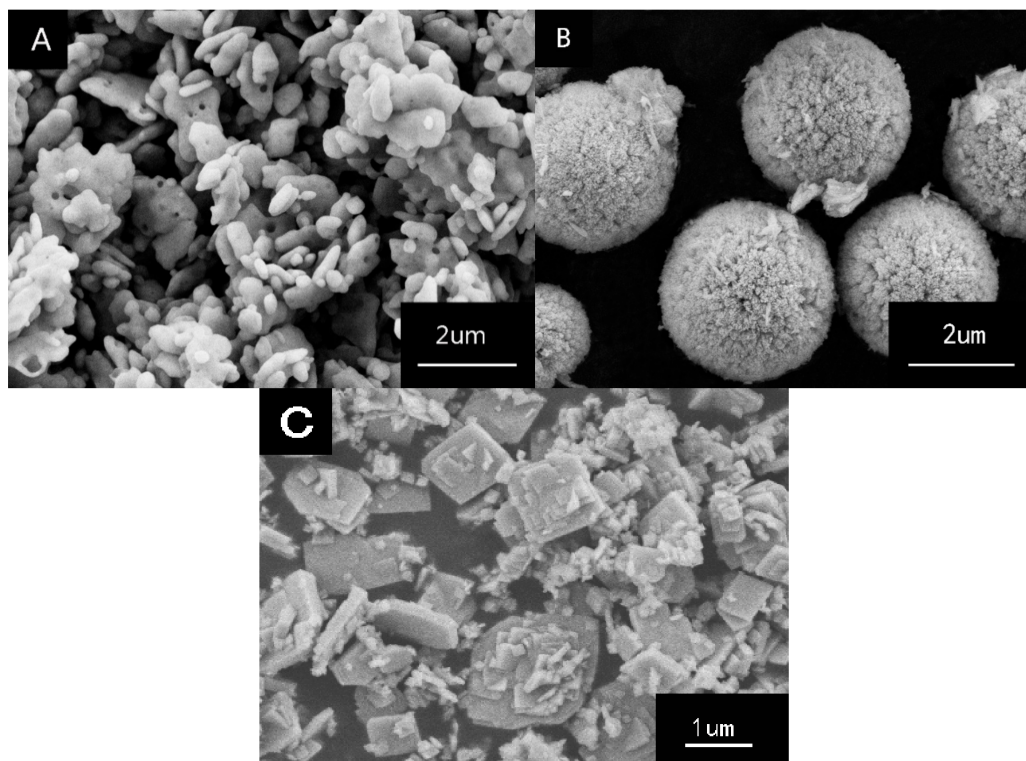


**Figure 1.** Scanning electron microscopy (SEM) images of barium sulphate ( $\text{BaSO}_4$ ): (A) in the presence of  $\text{BaCl}_2$  and  $\text{Na}_2\text{SO}_4$ , (B) in the presence of  $\text{BaCl}_2$ ,  $\text{Na}_2\text{SO}_4$  and ethylenediaminetetraacetic acid (EDTA), and (C) in the presence of  $\text{BaCl}_2$  and  $\text{Na}_2\text{S}_2\text{O}_8$ .

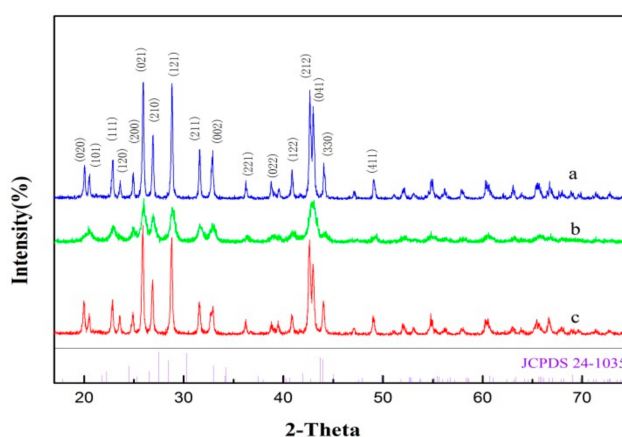


**Figure 2.** X-ray powder diffraction (XRD) pattern of  $\text{BaSO}_4$ : (a) in the presence of  $\text{BaCl}_2$  and  $\text{Na}_2\text{SO}_4$ , (b) in the presence of  $\text{BaCl}_2$ ,  $\text{Na}_2\text{SO}_4$ , and EDTA, and (c) in the presence of  $\text{BaCl}_2$  and  $\text{Na}_2\text{SO}_4$ .

### 3.1.2. Influence of Stirring Rate

The stirring rate has a large effect on the particle size of barium sulfate microspheres. Figure 3 gives the SEM image of barium sulfate prepared at a stirring rate of 0, 250, 500, and 750 r/min, respectively. At different stirring rates, the particle size of the barium sulfate microspheres was significantly different. The reason for this phenomenon was that there was a uniform distribution of

the solute in the solution at a high agitation rate, which caused the crystal nucleus to form more easily, the amount of crystal particles to increase, and the particle size to become smaller. However, when the stirring rate was too low, the size of the barium sulfate microspheres was different due to the uneven concentration of the solution after the addition of sodium sulfate. Therefore, the stirring rate can affect the size of the barium sulfate microspheres. In this experiment, the optimal experimental condition was a stirring rate of 250 r/min.

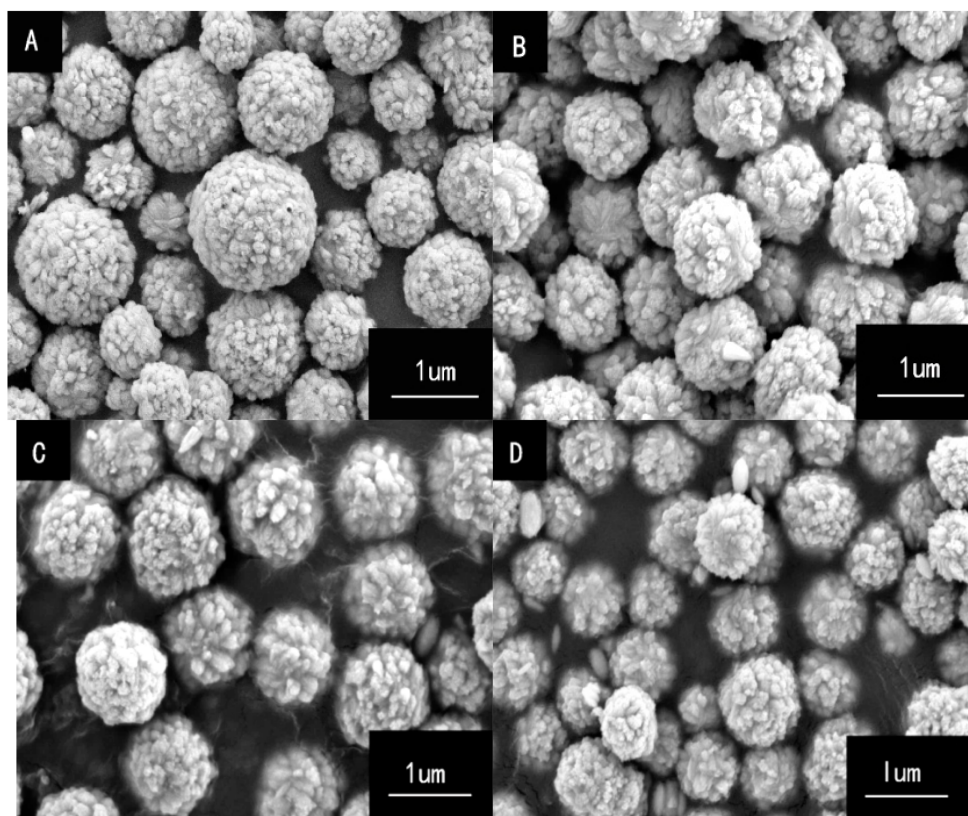


**Figure 3.** SEM of BaSO<sub>4</sub> at different stirring rates: (A) 0 r/min, (B) 250 r/min, (C) 500 r/min, (D) 750 r/min.

### 3.1.3. Influence of Temperature Reflex

The synthesis of barium sulfate microspheres is a crystallization reaction, so temperature has a certain influence on its formation and nucleation. The effect of different reaction temperature conditions on the crystallization of barium sulfate is shown in Figure 4. At 15 °C, the synthesized barium sulfate microspheres (Figure 5A) had a small particle size and were distributed unevenly. As the temperature increased, the barium sulfate sizes gradually increased. When the temperature was raised to 95 °C (Figure 4C), the barium sulfate particle size reached 3 μm. There are two main reasons for this phenomenon: (1) The complex will precipitate under low temperature conditions, which affects the complexing force of the complex on Ba<sup>2+</sup>. (2) In the low temperature region, it is advantageous to generate a large number of crystal nuclei to refine the barium sulfate particles. According to Equation (1), the growth rate of crystal has a strong relationship with temperature:

$$U_N = n\lambda v \exp(-\Delta G_{L \rightarrow S}/RT) [1 - \exp(-\Delta G_V/RT)] \quad (1)$$

where  $U_N$  is the nucleation rate,  $\lambda$  is the interatomic spacing,  $v$  is the transition frequency,  $n$  is the additional factor,  $T$  is the absolute temperature,  $-\Delta G_{L \rightarrow S}$  is the activity energy, and  $R$  is the Boltzmann constant (J/K<sup>-1</sup>) [22].

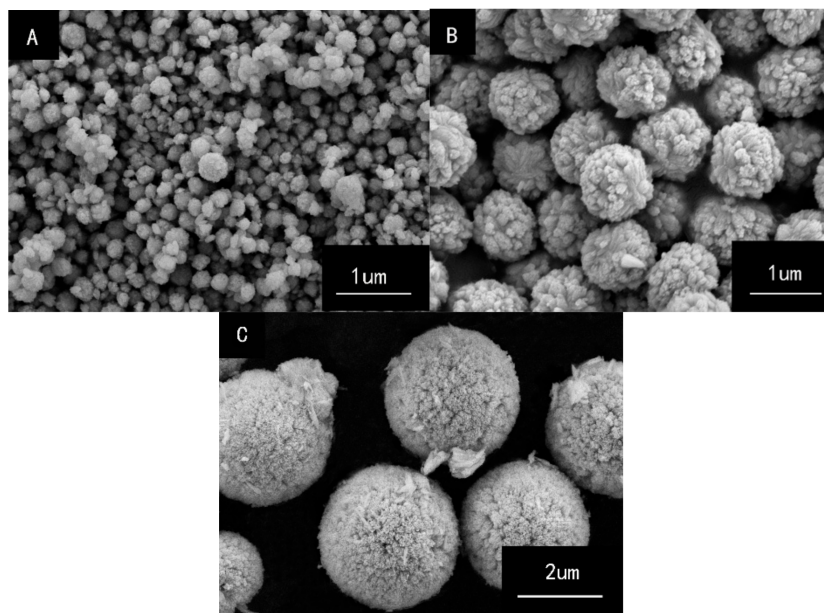


**Figure 4.** SEM of BaSO<sub>4</sub> at different reaction temperatures: (A) 15 °C, (B) 55 °C, (C) 95 °C.

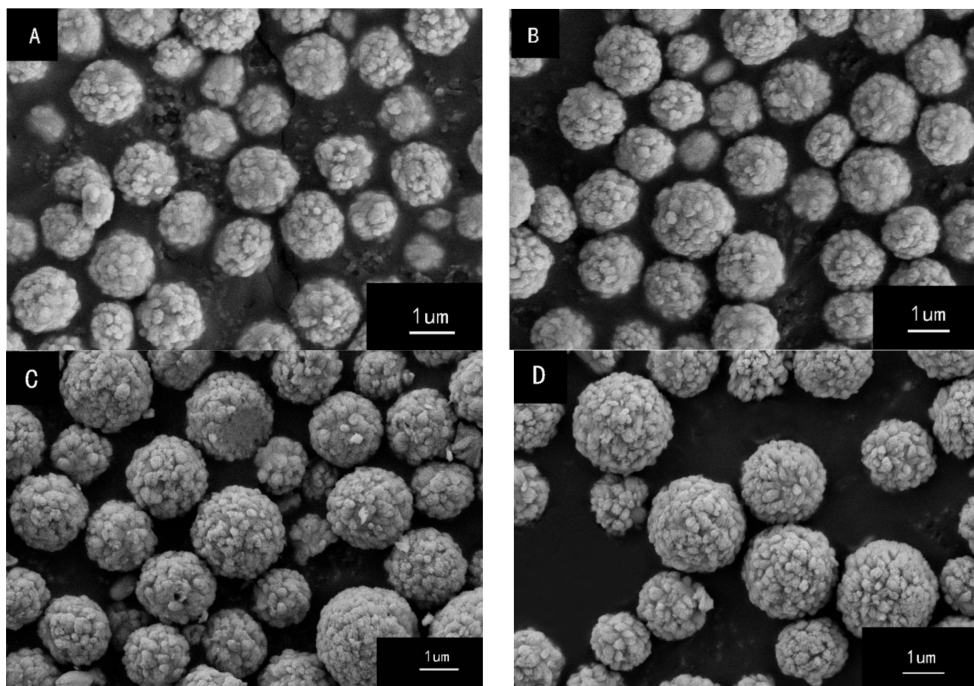


**Figure 5.** SEM of BaSO<sub>4</sub> at different Ostwald ripening times ((A) 0, (B) 1 h, (C) 1 day, (D) 7 days).

### 3.1.4. Influence of Ripening Time

Figure 5 shows barium sulfate particles at different ripening times. As the ripening time was prolonged, the surface of the barium sulfate microspheres became smoother and the particle size continued to increase, a result which was not obvious. After the ripening was further extended to seven days, the morphology and size of the barium sulfate product remained basically unchanged. According to the ripening mechanism, the solubility of smaller particles in solution was greater than that of the large particles. The crystal formation and dissolution were in a state of dynamic equilibrium under the supersaturation condition. This caused the small particles of barium sulfate to dissolve,

and the large particles gradually became larger. Thus, the new crystal nucleus was easy to deposit on the surface of the large particles to fill the surface defects. Therefore, as the ripening time increased, the surface of the microspheres tended to be smooth, as shown in Figure 5. However, the solubility of barium sulfate in water is small, so the ripening time does not significantly increase the particle size. After the ripening time reached one day, even if the Ostwald ripening time was increased, the particle size of the barium sulfate microspheres did not change substantially, and the particle surface of the barium sulfate microspheres remained unchanged (see Figure 6). Therefore, the best Ostwald ripening time is one day.

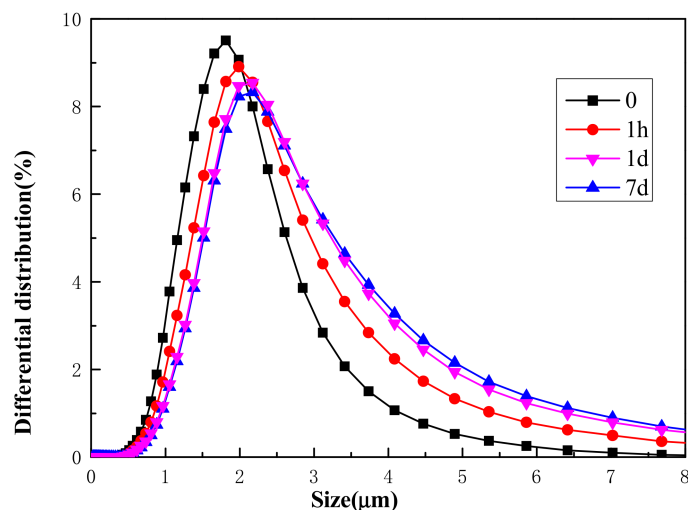


Figure 6. PSD of BaSO<sub>4</sub> at different Ostwald ripening.

### 3.2. Application

The next step was the application of the barium sulfate microspheres prepared under the above optimal conditions to the diffusion layer in the dry diagnosis of high-density lipoprotein. This step was divided into two parts: the preparation of the multifunctional layer and the application of the prepared multifunctional layer to the high-density lipoprotein dry film.

#### 3.2.1. BaSO<sub>4</sub> Multifunctional Layer

The multifunctional layers of high-density lipoprotein (HDL) dry tablets made with amorphous BaSO<sub>4</sub> powder and microspheres are shown in Figure 7.

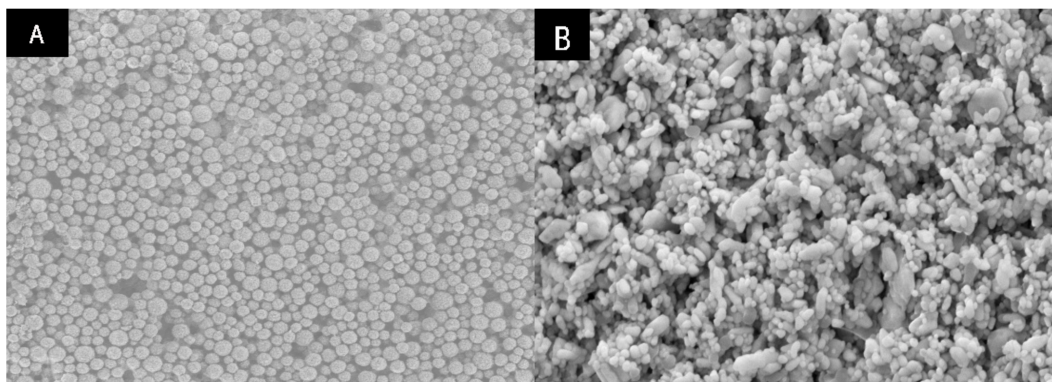
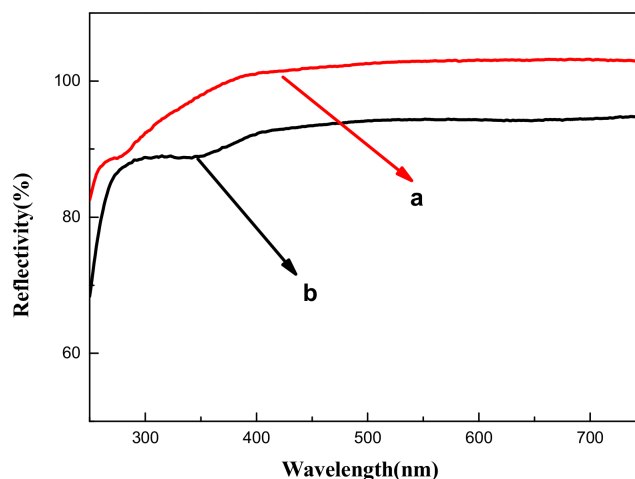


Figure 7. SEM micrographs of the BaSO<sub>4</sub> multifunctional layer with different BaSO<sub>4</sub> particles ((A) BaSO<sub>4</sub> microspheres, (B) amorphous BaSO<sub>4</sub>).

The diffuse reflectance measurement of coating samples of barium sulfate microspheres and commercially available barium sulfate was conducted using a UV-2600 (Shimadzu Corporation, Tokyo, Japan), as shown in Figure 8. It can be clearly seen that the barium sulfate microsphere produced in this paper has a higher diffuse reflection effect than that of the commercially available barium sulfate in the range of 400–780 nm of visible light wavelength, reaching more than 99%. Therefore, it can be applied to the diffusion layer of medical diagnostic dry films.



**Figure 8.** Reflectance spectrum: (a) homemade barium sulfate microspheres; (b) commercially available barium sulfate.

### 3.2.2. High-Density Lipoprotein Tablets

The  $\text{BaSO}_4$  multifunctional layer was applied to the dry chemical reagent layer of high-density lipoprotein, and the structure of high-density lipoprotein in vitro diagnostic reagent is shown in Figure 9. Repeatability and sensitivity are criteria for evaluating the dry films.

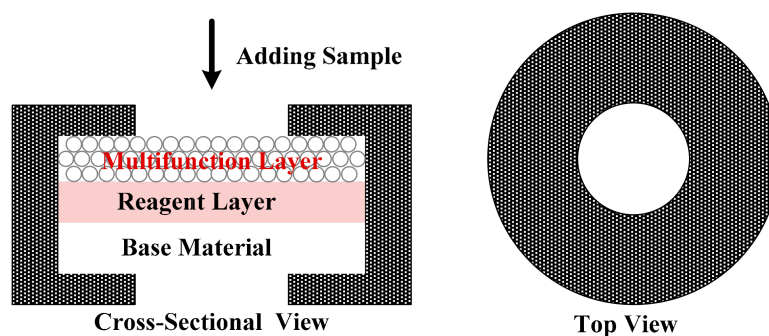


**Figure 9.** Structure of dry chemical diagnostic reagent in vitro.

#### (a) Reproducibility

Under the condition of 37 °C constant temperature, the serum was added to the high-density lipoprotein dry surface to test. The reaction time was five minutes, and the experiment was repeated five times. The results of five groups of experiments are shown in Figure 10. The reflectance densitometer detected the reflectance signal values of five groups of dry films, as shown in Table 1.

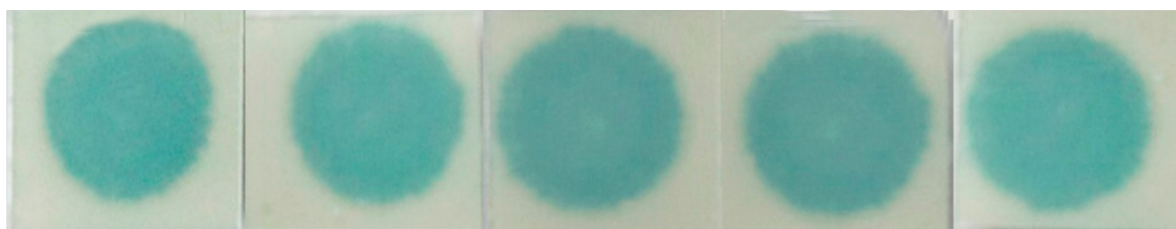


**Figure 10.** Image of dry chemical diagnostic reagents in vitro.

**Table 1.** Light reflection signal values of dry chemical diagnostic reagents in vitro.

Number	Value (V)	Average Value	Deviation (%)
1	0.3228		−0.0017
2	0.3297		0.0052
3	0.3255	0.3245	0.0010
4	0.3204		−0.0041
5	0.3239		−0.0004

As can be seen from Figure 10, the serum sample was filtered and diffused to the reagent layer by the BaSO<sub>4</sub> multifunctional layer that caused color after reaction. The reaction color was uniform, indicating that the serum sample could be uniformly diffused to the reagent layer in the BaSO<sub>4</sub> multifunctional layer. In addition, Table 2 illustrates that homemade BaSO<sub>4</sub> multi-function not only in the multifunctional layer uniform diameter distribution, the surface of the gap and the internal space is distributed evenly because of the small error ( $\pm 0.01\%$ ). Thus, for serum spreading, the BaSO<sub>4</sub> multifunctional layer can be further applied to in vitro diagnostic dry chemistry due to its repeatability.

**Table 2.** Light reflection signal values of dry chemical diagnostic reagents in different concentrations.

Concentration (mg/dL)	Value
110	0.3240
55	0.3773
27.5	0.4248
13.75	0.5037
6.875	0.5968

#### (b) Sensitivity

The results of the high-density lipoprotein samples with different concentrations are shown in the Figure 11. The depth of color was mainly related to the concentration of high-density lipoprotein in serum samples. The depth of dry film color with different concentrations could be detected by optical reflectance density meter. The darker the color of the dry film, the smaller the value of detection. The signal value of the dry film detected by the optical reflectance density meter is shown in Table 2. It shows an obvious change in the color gradient of high-density lipoprotein serum samples with different concentrations from left to right after the multifunctional layer diffusion and the color rendering reaction of the reagent layer. The color has deepened from left to right. At a 670 nm wavelength, there was a stronger capacity to absorb the light of the darker color. Therefore, the weaker the light was reflected to the detector, the smaller was the signal value, and vice versa. The optical reflectance signal values of the different high-density lipoprotein detected by the optical reflectometer are shown in Table 2. It can be seen that high-density lipoprotein dry tablets are highly sensitive to high-density lipoprotein serum samples of different concentrations, so the BaSO<sub>4</sub> multifunctional layer can be successfully applied to high-density lipoprotein dry tablets.

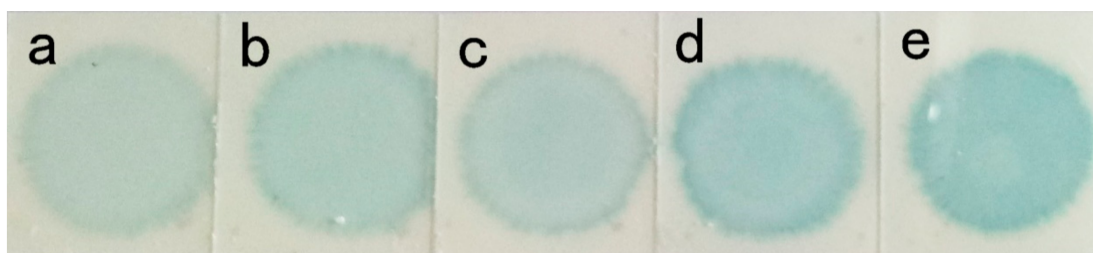


**Figure 11.** Image of different concentrations of HDL ((a) 6.875 mg/dL, (b) 13.75 mg/dL, (c) 27.5 mg/dL, (d) 55 mg/dL, (e) 110 mg/dL).

#### 4. Conclusions

This paper demonstrated that barium sulfate microspheres synthesized by the EDTA.2Na complex had a higher reflectivity compared with that of commercial barium sulfate, which can reduce the error caused by diffuse reflection during measurement. The authors further proved the important role of EDTA in the formation of barium sulfate particles using  $\text{Na}_2\text{S}_2\text{O}_8$ . The morphology of barium sulfate particles was characterized by XRD, PSD, and SEM. The barium sulfate microsphere produced in this study has a higher reflectivity than that of commercial barium sulfate, so it can be applied to the diffusion layer of biomedical dry films.

**Author Contributions:** Y.L., X.G. and H.J. conceived and designed the experiments; Y.L. performed the experiments; Y.L., Q.G. and G.H. analyzed the data; S.Y. contributed materials; Y.L. and H.J. wrote the paper.

**Funding:** Financial supported by the National Natural Science Foundation of China (91634101, 21601016), the Beijing Municipal Natural Science Foundation (2174073) and The Project of Construction of Innovative Teams and Teacher Career Development for Universities and Colleges under Beijing Municipality (IDHT20180508).

**Conflicts of Interest:** The authors declare no conflict of interest.

#### References

- Nagaraja, B.M.; Jung, K.D.; Ahn, B.S. Catalytic decomposition of  $\text{SO}_3$  over Pt/ $\text{BaSO}_4$  materials in sulfur-iodine cycle for hydrogen production. *Ind. Eng. Chem. Res.* **2009**, *48*, 1451–1457. [CrossRef]
- Gao, H.W.; Lin, J.; Li, W.Y. Formation of shaped barium sulfate-dye hybrids: Waste dye utilization for eco-friendly treatment of wastewater. *Environ. Sci. Pollut. Res.* **2010**, *17*, 78–83. [CrossRef] [PubMed]
- O'Connor, S.D.; Yao, J.; Summers, R.M. Lytic metastases in thoracolumbar spine: Computer-aided detection at CT-preliminary study. *Radiology* **2007**, *242*, 811–816. [CrossRef] [PubMed]
- Yao, C.; Yang, G. Synthesis, thermal, and rheological properties of poly (trimethylene terephthalate)/ $\text{BaSO}_4$  nanocomposites. *Polym. Adv. Technol.* **2009**, *20*, 768–774. [CrossRef]
- Ricker, A.; Liu-Snyder, P.; Webster, T.J. The influence of nano MgO and  $\text{BaSO}_4$  particle size additives on properties of PMMA bone cement. *Int. J. Nanomed.* **2008**, *3*, 125.
- Romero-Ibarra, I.C.; Rodriguez, G.G.; Garcia-Sanchez, M.F. Hierarchically nanostructured barium sulfate fibers. *Langmuir* **2010**, *26*, 6954–6959. [CrossRef] [PubMed]
- Li, M.; Colfen, H.; Mann, S.J. Crystal design of Barium Sulfate using double-hydrophilic block copolymers. *Angew. Chem. Int. Ed. Engl.* **2000**, *39*, 604–607.
- Hua, L.N.; Wang, G.X.; Cao, R. Fabrication and surface properties of hydrophobic barium sulfate aggregates based on sodium cocoate modification. *Appl. Surf. Sci.* **2014**, *315*, 184–189. [CrossRef]
- Barium Sulfate. Available online: <https://baike.so.com/doc/876966-7117269.html> (accessed on 25 July 2018).
- Gu, X.Y. Preliminary Study on Characteristics of Structure of Voids in Particle Assemblies Generated by PFC3D. Master's Thesis, Tsinghua University, Beijing, China, June 2009.
- Shi, H.M. Research on Permeability Characteristic of Porous Media of Pellets Packing. Master's Thesis, Northeastern University, Shenyang, China, June 2005.
- Han, L.M. Development of ultra-fine barium sulfate. *Inorg. Salt Ind.* **1993**, *2*, 29.

13. Li, J.; Liu, D.D. Effects of polyacrylic acid additive on barium sulfate particle morphology. *Mater. Chem. Phys.* **2016**, *175*, 180–187. [[CrossRef](#)]
14. Wang, M.; Wang, Y.J. Preparation of ultrafine barium sulfate particle using a water/oil microemulsion. *J. Tsinghua Univ. (Sci. Technol.)* **2002**, *42*, 1594–1597.
15. Liu, Y.Z.; Li, J.P. Preparation of barium sulfate nanoparticles. *J. Basic Sci. Eng.* **2001**, *9*, 2–3.
16. Uchida, M.; Sue, A.; Yoshioka, T.; Okuwaki, A. Hydrothermal synthesis of needle-like barium sulfate using a barium(ii)-edta chelate precursor and sulfate ions. *J. Mater. Sci. Lett.* **2000**, *19*, 1373–1374. [[CrossRef](#)]
17. Uchida, M.; Sue, A.; Yoshioka, T.; Okuwaki, A. Morphology of barium sulfate synthesized with barium(ii)-aminocarboxylate chelating precursors. *CrystEngComm* **2001**, *3*, 21–26. [[CrossRef](#)]
18. Jones, F.; Jones, P.; Ogden, M. The interaction of EDTA with barium sulfate. *J. Colloid Interface Sci.* **2007**, *316*, 553–561. [[CrossRef](#)] [[PubMed](#)]
19. Chen, Q.D.; Shen, X.H. Formation of mesoporous BaSO<sub>4</sub> microspheres with a larger pore size via Ostwald Ripening at room temperature. *Cryst. Growth Des.* **2010**, *10*, 3838–3842. [[CrossRef](#)]
20. Hua, L.N.; Wang, G.X.; Yang, C. Fabrication of submicron barium sulfate aggregates in the presence of ethylenediaminetetraacetic acid anions. *Particuology* **2015**, *22*, 157–162. [[CrossRef](#)]
21. Zhang, M.; Li, X.H.; Hu, Q.Y. Complex synthesis of barium sulfate particles. *Chin. J. Nonferrous Met.* **2009**, *19*, 1511–1516.
22. Zhao, Y.H.; Liu, J.R. Effect of EDTA and phosphate on particle size during precipitation of nanosized BaSO<sub>4</sub> particles. *Chem. Lett.* **2006**, *35*, 1040–1041. [[CrossRef](#)]
23. Holzwarth, U.; Gibson, N. The Scherrer equation versus the ‘Debye-Scherrer equation’. *Nat. Nanotechnol.* **2011**, *6*, 534. [[CrossRef](#)] [[PubMed](#)]
24. Piton, D.; Fox, R.O.; Marcant, B. Simulation of fine particle formation by precipitation using computational fluid dynamics. *Can. J. Chem. Eng.* **2010**, *78*, 983–993. [[CrossRef](#)]



© 2018 by the authors. Licensee MDPI, Basel, Switzerland. This article is an open access article distributed under the terms and conditions of the Creative Commons Attribution (CC BY) license (<http://creativecommons.org/licenses/by/4.0/>).